Reaction Mechanism of the Synthesis of Ammonia in the $N_2/H_2/BeO$ and $N_2/H_2/FeO$ Systems: A Theoretical Study

Der-Yan Hwang*,† and Alexander M. Mebel*,‡

Department of Chemistry, Tamkang University, Tamsui 25137, Taiwan, and Institute of Atomic and Molecular Sciences, Academia Sinica, P.O. Box 23-166, Taipei 10764, Taiwan

Received: February 18, 2003; In Final Form: April 26, 2003

Ab initio G2M(MP2)//MP2/6-31G** and density functional B3LYP/6-311+G(3df,2p)//B3LYP/6-31G** calculations for various reactions in the $N_2/H_2/BeO$ and $N_2/H_2/FeO$ systems show that beryllium and iron oxides can catalyze N_2 hydrogenation and the reaction mechanism involves a facile addition of H_2 to metal oxide to form HMOH, which reacts with nitrogen through N_2 insertion into the M−H bond. The insertion barrier decreases from 125.2 kcal/mol for the $N_2 + H_2$ reaction to 68.9 and 45.3 kcal/mol for N_2 + HBeOH and N_2 + HFeOH, respectively. After the formation of η^2-N_2(H)MOH intermediates, H atom can migrate from O to N with barriers of 59.2 and 50.7 kcal/mol leading to the N_2H_2MO complexes of metal oxides with diazene. The $MO + H_2 + N_2 \rightarrow N_2H_2MO$ reactions in the gas phase can easily occur providing that the chemically activated HMOH species formed at the first step do not dissipate their energy before they collide with the N_2 molecule. The second and third stages of nitrogen hydrogenation in the presence of a metal oxide have been investigated taking BeO as a model. The results indicate that the gas-phase $N_2H_2BeO + H_2 \rightarrow N_2H_4BeO$ and $N_2H_4BeO + H_2 \rightarrow 2NH_3 + BeO$ reactions can be facile because they exhibit the highest barriers of 10.4 and 13.4 kcal/mol, respectively, relative to the reactants.

Introduction

The reaction of nitrogen molecule with molecular hydrogen yielding ammonia is one of the most important processes of the chemical industry.[1] The heterogeneously catalyzed reaction was proposed by Fritz Haber, who received the Nobel Prize in chemistry in 1918.[2] The search for more efficient catalysts is an active field of research, but only a little progress has been made since Mittasch suggested iron oxide catalysts, which are still in use today.[1] Until now, most heterogeneous catalysts applied in the industry have been developed by trial-and-error experiments. In recent years, there has been a growing interest on the part of theorists to the catalyst design for the ammonia synthesis. It has been shown that the catalytic activity of metal surfaces correlates with their nitrogen absorption energy because this energy is related to the activation energy for N_2 dissociation on the surface,[3,4] which is considered to be the rate-limiting step.[5,6] Plane wave density functional calculations have been applied to obtain N_2 absorption energies at various metal surfaces (pure, bimetallic, or precovered by adsorbates), and on the basis of the calculated energies, predictions have been made on the efficiency of different metals for the catalytic synthesis of ammonia.[7,8]

Meanwhile, it is also important to understand the elementary reaction mechanism of nitrogen hydrogenation. Without a catalyst, the reaction of N_2 fixation and its reduction to NH_3 is thought to take place in three consequent steps:

$$N_2 + H_2 \rightarrow N_2H_2 \quad (1)$$

$$N_2H_2 + H_2 \rightarrow N_2H_4 \quad (2)$$

$$N_2H_4 + H_2 \rightarrow 2NH_3 \quad (3)$$

Our recent ab initio G2M(MP2)//MP2/6-31G** calculations[9] of potential energy surfaces for these three reactions have shown that all reaction steps are slow owing to high barriers for the molecular hydrogen additions. The three-center 1,1-H_2 additions are clearly preferable as compared to the four-center 1,2-additions. With respect to the initial $N_2 + H_2$ reactants and the most stable isomers of diazene, N_2H_2, and hydrazine, N_2H_4, the highest barriers on the reaction pathways for the addition of the first, second, and third H_2 molecules were found to be 125.2, 57.5, and 65.5 kcal/mol, respectively. Thus, the addition of the first H_2 was demonstrated to be the rate-determining stage of nitrogen hydrogenation.[9]

The goal of the present study is to investigate how the reaction mechanism, thermochemical parameters, and barrier heights for nitrogen hydrogenation change in the presence of a metal oxide, MO. Here, we have chosen two different metals, M, an alkaline-earth metal, beryllium, and a transition metal, iron. For $N_2/H_2/BeO$, which can be considered as a simpler model system, we investigate the entire reaction pathway from N_2 to NH_3, that is, the whole $N_2 + 3H_2 + BeO \rightarrow 2NH_3 + BeO$ reaction. It is well-known that beryllium oxide can readily react with molecular hydrogen producing HBeOH.[10−12] Moreover, our recent study of the $CO/H_2/BeO$ system demonstrated that the addition of molecular hydrogen to carbon monoxide with its conversion to formaldehyde can be significantly enhanced in the presence of BeO.[13] A similar effect could be also expected for the H_2 addition to N_2, N_2H_2, and N_2H_4.

Because the addition of the first hydrogen molecule is expected to be the rate-determining step both without and with the presence of a metal oxide, in the $N_2/H_2/FeO$ system, we investigate only the first step of nitrogen hydrogenation, $N_2 + H_2 + FeO \rightarrow N_2H_2FeO$. The iron oxide molecule is considered both in the ground electronic quintet $^5\Delta$ state (q-FeO) and an excited lowest triplet $^3\Sigma^-$ state (t-FeO).

† Tamkang University.
‡ Academia Sinica.

10.1021/jp034416l CCC: $25.00
Published on Web 06/03/2003

Although catalytic processes usually occur in solution or in a solid state, an approach to understanding their reaction mechanisms can start from the study of these reactions in the gas phase. For such study, ab initio calculations of PES represent an invaluable tool. Once the gas-phase reaction mechanisms are understood by means of theoretical and experimental studies, a comparison can be made between the reactions in the gas and condensed phases and the role of condensed-phase effects can be better comprehended. Thus, the gas-phase studies provide first steps toward a more detailed understanding of the role of electronic structure in the more complex systems involved in condensed-phase chemistry. In addition, the gas-phase reactions of neutral metal oxides can be studied experimentally using the matrix isolation infrared or Fourier-transform infrared (FTIR) spectroscopy, and in this view, theoretical calculations of PES give valuable information concerning the reaction mechanism, energetics, and vibrational spectra of the species involved, which can guide future experiments.

Computational Methods

Full geometry optimizations were run at the MP2/6-31G** level of theory[14] to locate various stationary points (reactants, intermediates, transition states, and products) on the ground singlet electronic state PES of the $N_2/H_2/BeO$ system. Harmonic vibrational frequencies were obtained at the MP2/6-31G** level to characterize the stationary points as minima (number of imaginary frequencies NIMAG = 0) or first-order saddle points (NIMAG = 1), to obtain zero-point vibrational energy corrections (ZPE), and to generate force constants needed for intrinsic reaction coordinate (IRC)[15] calculations. To predict more reliable ZPE, the raw calculated ZPE values were scaled by 0.967 to account for their average overestimation.[16] The IRC method[15] was used to track minimum energy paths from transition structures to the corresponding minimum. A step size of 0.1 amu$^{1/2}$ bohr or larger was used in the IRC procedure. The relative energies were refined using single-point calculations with MP2/6-31G**-optimized geometry employing the G2M(MP2) method,[17] a modification of G2(MP2)[18−21] in which QCISD(T)/6-311G** calculations are replaced by the coupled cluster[22] CCSD(T)/6-311G** calculations. Such G2M(MP2)//MP2/6-31G** approach should provide reliable structures of the reactants, products, intermediates, and transition states, as well as their chemically accurate energies (within ~0.1 eV).[17−21]

For the $N_2/H_2/FeO$ system, geometries of various species were optimized using the hybrid density functional B3LYP approach[23,24] with the all-electron 6-31G** basis set. Calculations of vibrational frequencies and IRC calculations were carried out at the same B3LYP/6-31G** level of theory. Relative energies were then refined by B3LYP computations with a large and flexible all-electron 6-311+G(3df,2p) basis set, which can be more correctly designated as 6-311+G(3fg) for the Fe atom because it includes three polarization f functions and a g function in addition to valence and diffuse s, p, and d functions. It is well-known that multireference MRCI calculations with large active spaces and basis sets are the most reliable way to provide chemical accuracy for the molecules containing transition metal atoms. Unfortunately, such calculations are extremely demanding computationally and are not feasible for the $N_2/H_2/FeO$ system. According to the literature,[25−27] the DFT B3LYP approach is a viable alternative method, which can give relative energies of various structures at least with semiquantitative accuracy. For instance, the B3LYP-calculated bond strength in the FeO($^5\Delta$) molecule, 91.7 kcal/mol, closely agrees with the experimental value of 92.9 ± 3.0 kcal/mol.[26] Also, the energy splitting between the $^5\Delta$ and $^3\Sigma^-$ electronic states of FeO is computed to be 27.9 and 24.7 kcal/mol at the B3LYP and MRCI levels, respectively, with the 6-311+G(3df,2p) basis set. Here, the internally contracted MRCI calculations[28,29] were carried out for FeO with the full valence (14,10) active space, and the Davidson correction for quadruple excitations was taken into account. Because we do not expect to achieve chemical accuracy for the $N_2/H_2/FeO$ system, the effects of spin−orbit coupling were not included in the present calculations. These effects are believed to be larger in isolated atoms than in molecules. For the iron atom in its ground ^{5}D state, the energy splitting due to the spin−orbit coupling reaches 978 cm^{-1},[30] that is, only 2.8 kcal/mol. An effect of this size does not exceed the anticipated accuracy of the present calculations, so we have chosen to neglect the spin−orbit coupling corrections at this stage.

To make a comparison between the $N_2/H_2/BeO$ and $N_2/H_2/FeO$ systems possible, we additionally carried out B3LYP/6-311+G(3df,2p) calculations for the $N_2 + H_2 + BeO \rightarrow N_2H_2BeO$ reaction. Most of the ab initio calculations described here were performed employing the Gaussian 98 package,[31] and for some of them, we used the MOLPRO 2000 program.[32]

Results and Discussion

$N_2/H_2/BeO$ System. ZPE-corrected relative energies of various species in the $N_2/H_2/BeO$ system calculated at the MP2/6-31G**, MP2/6-311G**, CCSD(T)/6-311G**, MP2/6-311+G(3df,2p), G2M(MP2), and B3LYP/6-311+G(3df,2p) levels of theory are listed in Table 1. Table 2 presents unscaled MP2/6-31G** calculated vibrational frequencies. The potential energy diagram along various reaction pathways computed at the G2M(MP2) level is shown in Figure 1, in which the panels a, b, and c correspond to the $BeO + H_2 + N_2$, $N_2H_2BeO + H_2$, and $N_2H_4BeO + H_2$ reactions, respectively. The optimized geometries of various compounds along the predicted reaction pathways are depicted in Figure 2.

$N_2 + H_2 + BeO \rightarrow N_2H_2BeO$ Reaction. Beryllium oxide can easily react with molecular hydrogen initially forming without a barrier the H_2BeO molecular complex stabilized by ~16 kcal/mol relative to the reactants and then rearranging to the HBeOH molecule via a low barrier with a transition state lying ~12 kcal/mol below $BeO + H_2$.[12] According to our most accurate G2M calculations, HBeOH resides 88.2 kcal/mol lower in energy than the reactants. BeO can also form a strong complex with N_2 bound by 26.3 kcal/mol at the G2M level and by 30.0 kcal/mol according to MP4/6-311G(2df,2pd)//MP2/6-31G** calculations by Frenking et al.[33] However, the $NNBeO + H_2 \rightarrow N_2 + HBeOH$ reaction is highly exothermic, so molecular hydrogen is likely to replace N_2 in the complex. Indeed, NNBeO can react with H_2 via transition state TS1 with a low barrier of 9.1 kcal/mol, and the reaction leads to the N_2−Be(H)OH complex. The latter is very weak and is bound with respect to $HBeOH + N_2$ only by ~0.2 kcal/mol.

The next reaction stage is insertion of N_2 into the H−Be bond of HBeOH proceeding to a *cis*-η^2-N_2(H)BeOH intermediate via transition state TS2a. The transition state lies 19.3 kcal/mol below the initial $BeO + N_2 + H_2$ reactants and only 7.0 kcal/mol higher in energy than $NNBeO + H_2$. The *cis*-η^2-N_2(H)BeOH readily isomerizes to *trans*-η^2-N_2(H)BeOH by rotation around the single Be−O bond through TS3 with a low barrier of 1.5 kcal/mol. At the next reaction step, the second H atom of *trans*-η^2-N_2(H)BeOH migrates from oxygen to the hydrogen-free nitrogen through a planar five-member ring transition state TS4. The process leads to the formation of N_2H_2BeO, a molecular complex of beryllium oxide and *trans*-HNNH.

TABLE 1: ZPE and ZPE-Corrected Relative Energies (kcal/mol) of Various Species in the N_2/H_2/BeO System Calculated at the MP2/6-31G, MP2/6-311G**, CCSD(T)/6-311G**, MP2/6-311+G(3df,2p), G2M(MP2), and B3LYP/6-311+G(3df,2p) Levels of Theory[a]**

	MP2/ 6-31G**		MP2/ 6-311G**	CCSD(T)/ 6-311G**	MP2/ 6-311+G(3df,2p)	G2M(MP2)	B3LYP/ 6-311+G(3df,2p)
species	ZPE	rel energy	rel energy	rel energy	rel energy	rel energy	rel energy
BeO + H_2 + N_2	11.69	0.0	0.0	0.0	0.0	0.0	0.0
HBeOH + N_2	16.05	−82.63	−85.22	−88.44	−85.02	−88.25	−90.64
NNBeO + H_2	13.92	−27.04	−28.00	−28.38	−25.91	−26.29	
TS1	16.34	−15.27	−16.73	−16.74	−17.21	−17.22	
N_2−Be(H)OH	16.91	−83.29	−86.21	−89.30	−85.31	−88.40	
TS2a	16.99	0.65	−2.57	−14.29	−7.62	−19.34	−27.80
cis-η^2-N_2(H)BeOH	21.6	−41.13	−42.88	−50.21	−45.82	−53.15	−57.78
TS3	20.93	−39.47	−40.98	−48.11	−44.55	−51.68	−56.00
trans-η^2-N_2(H)BeOH	21.72	−41.91	−43.54	−50.74	−46.3	−53.50	−57.42
TS4	20.18	17.09	17.55	10.02	13.25	5.71	−0.03
TS2b	20.05	57.58	57.28	49.97	53.55	46.23	
N_2H_2BeO	23.21	6.91	5.56	−1.06	5.73	−0.88	−7.74
BeO + *trans*-HNNH	20.00	57.75	58.23	52.67	54.42	48.86	
N_2H_2BeO + H_2	29.8	6.91	5.56	−1.06	5.73	−0.88	
HBeOH + *trans*-HNNH	30.95	−24.88	−26.99	−35.77	−30.60	−39.39	
TS5	32.44	19.50	17.57	11.51	15.59	9.53	
HNN(H)Be(H)OH	34.69	−42.89	−45.87	−54.43	−47.94	−56.50	
TS6	34.12	−4.15	−7.05	−16.00	−11.09	−20.04	
H_2NN(H)BeOH	37.38	−63.24	−67.35	−71.87	−73.65	−78.17	
TS7	36.02	1.37	0.74	−1.45	−6.29	−8.48	
N_2H_4BeO	39.54	−21.45	−24.25	−27.28	−26.07	−29.10	
BeO + N_2H_4	36.12	40.54	40.58	37.25	33.79	30.46	
N_2H_4BeO + H_2	46.13	−21.45	−24.25	−27.28	−26.07	−29.10	
HBeOH + N_2H_4	47.07	−42.09	−44.64	−51.19	−51.23	−57.79	
TS8	48.91	−10.62	−12.81	−16.07	−19.05	−22.31	
N_2H_4Be(H)OH	50.57	−62.24	−66.19	−72.47	−70.49	−76.77	
TS9	46.63	6.23	1.79	−11.16	−2.77	−15.72	
H_2NBe(NH_3)OH	51.26	−130.17	−135.07	−137.89	−143.22	−146.03	
NH_3 + H_2NBeOH	47.78	−107.06	−112.98	−115.92	−121.50	−124.43	
TS10 + NH_3	46.94	−41.15	−41.96	−42.71	−51.40	−52.15	
H_3NBeO + NH_3	50.35	−64.58	−67.51	−68.75	−71.06	−72.29	
BeO + 2NH_3	46.49	−3.04	−4.23	−5.64	−14.37	−15.78	

[a] All relative energies are given with respect to BeO + N_2 + nH_2 with n = 1, 2, or 3.

Although the hydrogen shift depicts a barrier of 59.2 kcal/mol relative to *trans*-η^2-N_2(H)BeOH, TS4 lies only 5.7 kcal/mol above BeO + N_2 + H_2.

An alternative reaction mechanism leads from HBeOH + N_2 directly to N_2H_2BeO by a concerted dihydrogen transfer via a late transition state TS2b. This process cannot compete with the three-step mechanism described above because the calculated barrier at TS2b relative to HBeOH + N_2 is as high as 134.4 kcal/mol. The N_2H_2BeO complex can dissociate to BeO + *trans*-HNNH with an energy loss of 49.8 kcal/mol and without an exit barrier. However, as will be seen in the subsequent section, N_2H_2BeO serves as an initial reactant for the second stage of nitrogen hydrogenation and can react with a second H_2 molecule.

The considerable reduction of the barrier for the H_2 addition to N_2 in the presence of BeO can be attributed to the fact that in the N_2 + H_2 reaction the nitrogen molecule has to insert into a very strong H−H bond (∼103 kcal/mol[34,35]) but in N_2 + HBeOH the insertion occurs into an one-half as strong Be−H bond (∼53 kcal/mol in BeH[35]). The N_2 + H_2 + BeO → N_2H_2-BeO reaction in the gas phase could be facile if BeO first reacts with molecular hydrogen and then hot, chemically activated HBeOH reacts with N_2. Alternatively, BeO can initially react with N_2 and then NNBeO can react with H_2. This also leads to the formation of chemically activated HBeOH + N_2 pair because the complex between them is very weak. On the contrary to the ∼49 kcal/mol endothermic N_2 + H_2 → *trans*-HNNH reaction, N_2 + H_2 + BeO → N_2H_2BeO is slightly exothermic (0.9 kcal/mol) and the highest barrier at TS4 is only 5.7 kcal/mol relative to the initial reactants. Thus, the reaction is likely to produce the N_2H_2BeO complex if the energy of chemically activated HBeOH + N_2 is not dissipated.

As seen in Table 1, relative energies of various intermediates and transition states of the N_2 + H_2 + BeO → N_2H_2BeO reaction calculated at the B3LYP/6-311+G(3df,2p) level agree with those obtained at the most reliable G2M(MP2) level within 2−8 kcal/mol. The largest deviation is found for TS2a, for which the B3LYP energy underestimates the G2M(MP2) value by 8.5 kcal/mol. For the transition states, we also carried out B3LYP/6-31G** geometry optimization, but their B3LYP/6-311+G(3df,2p)//B3LYP/6-31G** energies differ from the B3LYP/6-311+G(3df,2p)//MP2/6-31G** energies by less than 0.1−0.2 kcal/mol.

N_2H_2BeO + H_2 → N_2H_4BeO Reaction. The reaction of N_2H_2-BeO with H_2 produces a HNN(H)Be(H)OH intermediate as the BeO fragment inserts into the H−H bond of molecular hydrogen. This process occurs via TS5 and has a low barrier of only 10.4 kcal/mol. Alternatively, HNN(H)Be(H)OH, which is a molecular complex of diazene with HBeOH, can be formed in the barrierless HBeOH + *trans*-HNNH reaction exothermic by 17.1 kcal/mol. At the next step, the hydrogen atom bound to Be in HNN(H)Be(H)OH migrates to the nitrogen of *trans*-HNNH via a four-member ring transition state TS6 (20.0 kcal/mol below the reactants) to produce a H_2NN(H)BeOH molecule. The other hydrogen bound to oxygen in H_2NN(H)BeOH migrates to the second nitrogen to give an N_2H_4BeO complex again through a four-member ring TS7, which resides 8.5 kcal/mol lower in energy than N_2H_2BeO + H_2.

TABLE 2: Vibrational Frequencies (cm^{-1}) of Various Compounds in the $N_2/BeO/H_2$ System Calculated at the MP2/6-31G Level**

species	frequencies
NNBeO	129, 129, 382, 382, 422, 1518, 2162
TS1	806i, 97, 127, 252, 279, 389, 1010, 1072, 1377, 2113, 2189, 2525
N_2−Be(H)OH	41, 57, 59, 160, 217, 437, 571, 634, 1187, 2177, 2242, 4042
TS2a	1177i, 173, 201, 244, 464, 487, 539, 721, 1450, 1533, 2020, 4051
cis-η^2-N_2(H)BeOH	275, 288, 324, 527, 601, 669, 821, 1366, 1410, 1503, 3318, 4009
TS3	353i, 270, 308, 489, 508, 607, 818, 1365, 1412, 1491, 3303, 4070
trans-η^2-N_2(H)BeOH	278, 287, 358, 538, 591, 709, 826, 1360, 1414, 1501, 3329, 4003
TS4	1524i, 364, 433, 623, 737, 767, 1390, 1432, 1451, 1571, 1920, 3429
TS2b	365i, 176, 189, 294, 533, 1221, 1404, 1466, 1501, 1610, 2427, 3205
N_2H_2BeO	92, 192, 441, 540, 610, 1315, 1374, 1536, 1586, 1620, 3427, 3501
TS5	860i, 100, 155, 239, 350, 587, 606, 880, 1136, 1328, 1357, 1414, 1590, 1611, 2018, 2452, 3370, 3497
HNN(H)Be(H)OH	101, 160, 335, 432, 560, 561, 669, 702, 834, 1143, 1345, 1347, 1600, 1609, 2026, 3372, 3488, 3984
TS6	709i, 166, 324, 420, 455, 591, 643, 798, 970, 1213, 1280, 1336, 1369, 1573, 1825, 3457, 3479, 3969
H_2NN(H)BeOH	123, 183, 280, 308, 452, 522, 606, 674, 972, 1159, 1323, 1411, 1517, 1709, 3547, 3652, 3695, 4018
TS7	1557i, 182, 291, 335, 525, 763, 811, 978, 1174, 1301, 1358, 1394, 1486, 1709, 2122, 3548, 3561, 3660
N_2H_4BeO	96, 186, 258, 405, 546, 751, 938, 1148, 1214, 1324, 1417, 1568, 1696, 1726, 3514, 3569, 3616, 3688
TS8	766i, 107, 138, 184, 327, 453, 558, 688, 937, 971, 1071, 1176, 1208, 1317, 1379, 1462, 1684, 1736, 2055, 2604, 3348, 3544, 3627, 3640
N_2H_4Be(H)OH	38, 211, 257, 279, 373, 487, 539, 669, 728, 804, 995, 1121, 1158, 1172, 1327, 1512, 1669,1729, 2011, 3515, 3540, 3613, 3632, 3995
TS9	778i, 174, 218, 251, 303, 422, 482, 584, 636, 689, 761, 789, 929, 1017, 1037, 1202, 1585, 1607, 1714, 3460, 3499, 3590, 3679, 3988
H_2NBe(NH_3)OH	26, 193, 198, 266, 297, 334, 433, 486, 602, 688, 697, 722, 937, 1254, 1279, 1638, 1698, 1706, 3554, 3673, 3705, 3711, 3772, 3985
H_2NBeOH	264, 290, 314, 335, 619, 709, 715, 1489, 1622, 3693, 3797, 4015
TS10	1597i, 429, 549, 726, 768, 875, 1387, 1432, 1605, 2120, 3632, 3748
H_3NBeO	207, 208, 536, 749, 749, 1337, 1567, 1701, 1701, 3542, 3678, 3679

The gas-phase $N_2H_2BeO + H_2 \rightarrow N_2H_4BeO$ reaction is expected to be facile and more efficient than the *trans*-HNNH + $H_2 \rightarrow NNH_2 + H_2 \rightarrow N_2H_4$ reaction, because the highest barrier for the former is only 10.4 kcal/mol with respect to the reactants, as compared to 57.5 kcal/mol for the latter.[9] N_2H_4BeO can dissociate to hydrazine and beryllium oxide without an exit barrier and with endothermicity of 59.6 kcal/mol. However, N_2H_4BeO can react with another H_2 molecule and serves as a precursor for the third stage of the nitrogen hydrogenation reaction.

$N_2H_4BeO + H_2 \rightarrow 2NH_3 + BeO$ Reaction. The addition of H_2 to N_2H_4BeO depicts a relatively low barrier of 6.8 kcal/mol located at TS8 and results in the N_2H_4Be(H)OH molecular complex of HBeOH with hydrazine. The dissociation energy of the complex to HBeOH + N_2H_4 is computed as 19.0 kcal/mol. N_2H_4Be(H)OH undergoes a 1,3-H migration from Be to a nitrogen atom in N_2H_4 through TS9, which lies 13.4 kcal/mol above the initial reactants, $N_2H_4BeO + H_2$. The hydrogen shift is accompanied with the break of the N−N bond so that the reaction product is an H_2NBe(NH_3)OH complex bound through a Be−N bond, which decomposes to H_2NBeOH + NH_3 without an exit barrier. The H_2NBeOH species can in turn undergo another 1,3-H migration from the O to N atom producing a H_3NBeO complex via TS10 (23.1 kcal/mol below $N_2H_4BeO + H_2$), which finally can dissociate to NH_3 + BeO. For the gas-phase N_2H_4 + HBeOH reaction, the highest barrier on the reaction pathway, 13.4 kcal/mol, is found at TS9 and the activation energy required to form the final BeO + $2NH_3$ products is 13.3 kcal/mol.

The overall pathway of the $N_2 + 3H_2 \rightarrow 2NH_3$ reaction catalyzed by beryllium oxide can be summarized as follows: BeO + H_2 + $N_2 \rightarrow$ NNBeO + H_2 (−26.3) → TS1 (−17.2) → N_2−Be(H)OH (−88.4) → TS2a (−19.3) → *cis*-η^2-N_2(H)BeOH (−53.2) → TS3 (−51.7) → *trans*-η^2-N_2(H)BeOH (−53.5) → TS4 (5.7) → N_2H_2BeO (−0.9), $N_2H_2BeO + H_2$ (−0.9) → TS5 (9.5) → HNN(H)Be(H)OH (−56.5) → TS6 (−20.0) → H_2NN(H)BeOH (−78.2) → TS7 (−8.5) → N_2H_4BeO (−29.1), $N_2H_4BeO + H_2$ (−29.1) → TS8 (−22.3) → N_2H_4Be(H)OH (−76.8) → TS9 (−15.7) → H_2NBe(NH_3)OH (−146.0) → H_2NBeOH + NH_3 (−124.4), H_2NBeOH (−124.4) → TS10 (−52.2) → H_3NBeO (−72.3) → BeO + NH_3 (−15.8), where the numbers in parentheses show relative energies (in kcal/mol) of various species with respect to the initial reactants.

N_2/H_2/FeO System. ZPE-corrected relative energies of various species in the N_2/H_2/FeO system calculated at the B3LYP/6-31G** and B3LYP/6-311+G(3df,2p) theoretical levels are collected in Table 3, while Table 4 shows unscaled B3LYP/6-31G** calculated vibrational frequencies. The potential energy diagram along various reaction pathways computed at the B3LYP/6-311+G(3df,2p)//B3LYP/6-31G** + ZPE(B3LYP/6-31G**) level is shown in Figure 3, and the optimized geometries of various compounds along reaction pathways are depicted in Figure 4.

$N_2 + H_2 + FeO \rightarrow$ trans-N_2H_2 + FeO Reaction in Quintet Electronic State. In general, the mechanism of the $N_2 + H_2$ + FeO reaction is similar to that with beryllium oxide, but the energetics and some details differ. As was found earlier,[27] iron oxide in its ground $^5\Delta$ electronic state reacts with molecular hydrogen to produce q-HFeOH (here and below, the prefixes "q" and "t" denote quintet and triplet electronic state species, respectively) overcoming a barrier of 12−13 kcal/mol. The addition of H_2 to FeO was calculated to be 46.3 kcal/mol exothermic at the B3LYP/6-311+G(3df,2p) level.[27] Next, q-HFeOH can react with the nitrogen molecule producing a q-*cis*-η^2-N_2(H)FeOH intermediate via transition state q-TS1a. The reaction occurs by insertion of N_2 into the Fe−H bond with formation of new N−H and Fe−N bonds. In contrast to the N_2/H_2/BeO system, where the transition state TS2a exhibits a three-center character, q-TS1 has a four-member ring structure, in which the newly formed N−H and Fe−N bonds involve two different nitrogen atoms. The calculated barrier at q-TS1, 45.3

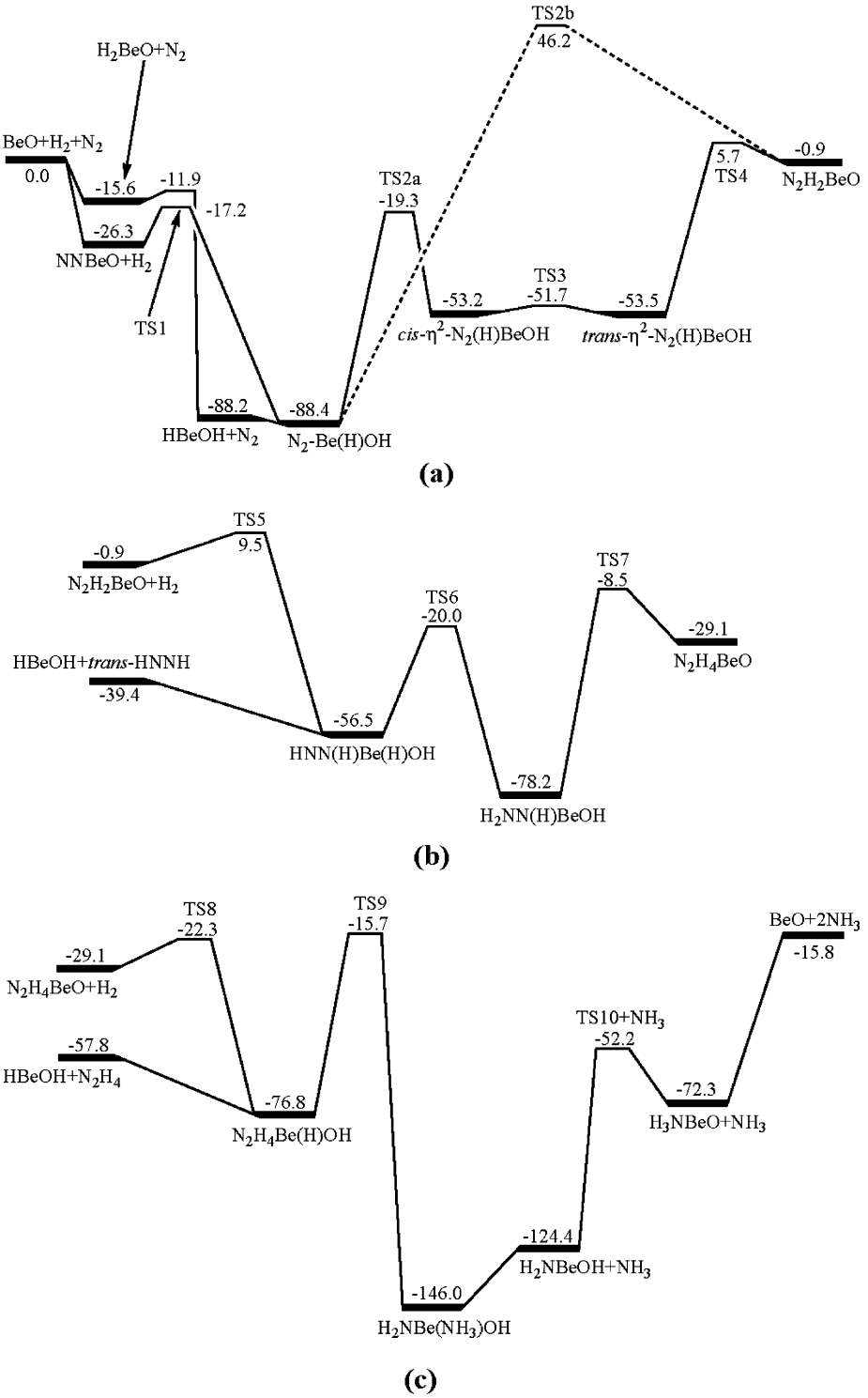

Figure 1. Potential energy diagrams of various reactions in the $N_2/H_2/BeO$ system calculated at the G2M(MP2)//MP2/6-31G** level of theory: (a) BeO + H_2 + N_2 → N_2H_2BeO reaction; (b) N_2H_2BeO + H_2 → N_2H_4BeO reaction; (c) N_2H_4BeO + H_2 → BeO + $2NH_3$ reaction. All relative energies are given in kcal/mol.

kcal/mol, is significantly lower than the barrier for N_2 insertion into the Be−H bond in HBeOH, 62.8 kcal/mol at the same B3LYP level. This result can be rationalized by the fact that the Fe−H bond (∼43 kcal/mol[34]) is somewhat weaker than the Be−H bond (∼53 kcal/mol[35]) and also by a less-strained character of the four-member ring transition state q-TS1 as compared to the three-center TS2a for the N_2 + HBeOH reaction. The N_2 + q-HFeOH → q-*cis*-η^2-N_2(H)FeOH reaction step is computed to be 42.8 kcal/mol endothermic, which is somewhat higher than the endothermicity of the N_2 + HBeOH → *cis*-η^2-N_2(H)BeOH process, 32.9 kcal/mol at the same level of theory. The structures of q-*cis*-η^2-N_2(H)FeOH and *cis*-η^2-N_2(H)BeOH differ; in the latter, the Be atom is bound to both nitrogens forming a BeN_2 three-member ring and there is no interaction between Be and H, while in the former, only one Fe−N bond is present and the iron atom additionally interacts with nitrogen's hydrogen. This agostic Fe−H bonding interaction typical for transition metals is characterized by a relatively short Fe−H distance of 2.000 Å and elongated N−H bond, 1.131 vs 1.02−1.04 Å for a regular N−H bond. Due to the

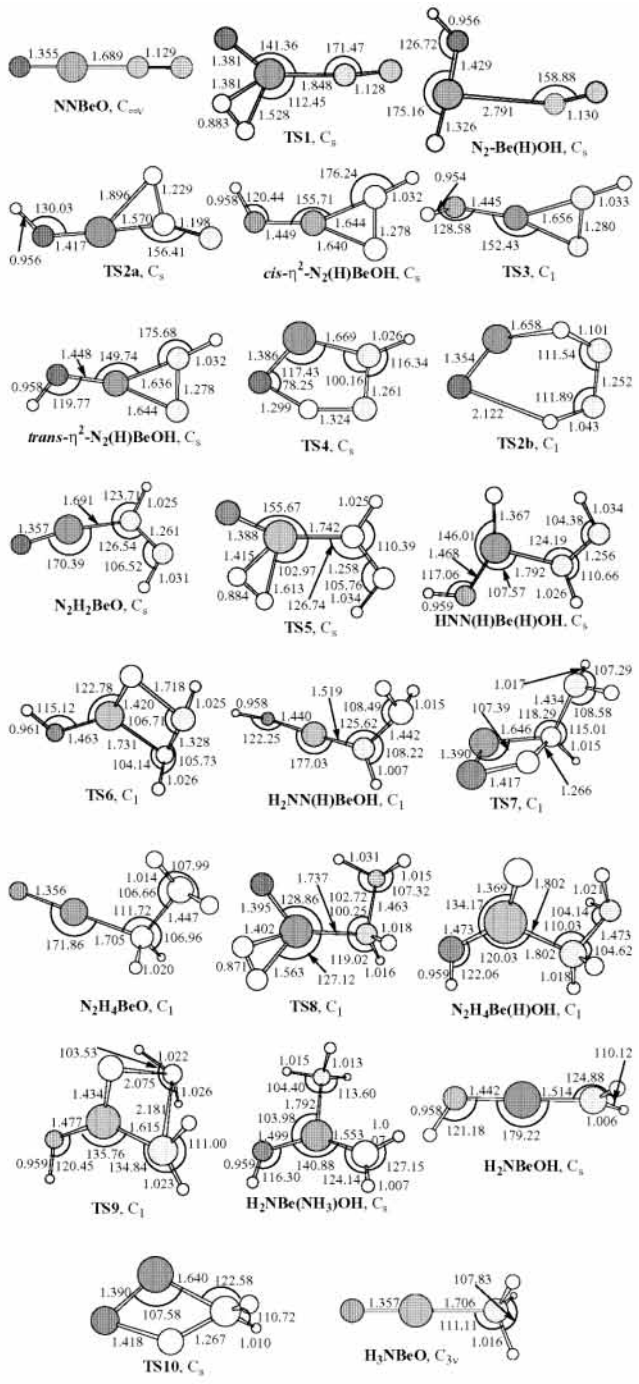

Figure 2. Geometries of intermediates and transition states of various reactions in the N_2/H_2/BeO system optimized at the MP2/6-31G** level of theory. Bond lengths are in Å and bond angles are in deg.

presence of the Fe−H bond, q-*cis*-η^2-N_2(H)FeOH acquires the four-member ring geometry.

The next reaction step is the q-*cis*-η^2-N_2(H)FeOH → q-*trans*-η^2-N_2(H)FeOH isomerization occurring via transition state q-TS2 with a relatively low 6.0 kcal/mol barrier. The isomerization in the N_2/H_2/FeO system is a more complicated process than that for N_2/H_2/BeO because, in addition to the rotation around the single Fe−O bond, it involves rotation around the N−N bond leading to the rupture of the agostic Fe−H bond and formation of the second Fe−N bond and a three-member FeN_2 cycle in q-*trans*-η^2-N_2(H)FeOH, so the barrier increases by 4.2 kcal/mol as compared to the corresponding value for the N_2/H_2/BeO system. As the agostic Fe−H bond is replaced by a stronger Fe−N bond, the q-*cis*-η^2-N_2(H)FeOH → q-*trans*-η^2-N_2(H)FeOH reaction is calculated to be 9.5 kcal/mol exothermic, on the contrary to the nearly thermoneutral *cis*-η^2-N_2(H)BeOH → *trans*-η^2-N_2(H)BeOH process.

From q-*trans*-η^2-N_2(H)FeOH, the reaction proceeds to a q-N_2H_2FeO molecular complex by hydrogen migration via a five-member ring transition state q-TS3. The structure of the planar q-TS3 is similar to that of TS4 in the N_2/H_2/BeO system. The calculated barrier height at q-TS3 is 50.7 kcal/mol, 6.7 kcal/mol lower than the barrier for the *trans*-η^2-N_2(H)BeOH → N_2H_2-BeO reaction, in line with the fact that the latter is more endothermic [by 49.7 kcal/mol at B3LYP/6-311+G(3df,2p)] as compared to the q-*trans*-η^2-N_2(H)FeOH → N_2H_2FeO isomerization process (38.1 kcal/mol). The decomposition of the N_2H_2-FeO complex to *trans*-HNNH + FeO proceeds with an energy loss of ∼22 kcal/mol but without an exit barrier.

The calculated barriers for individual reaction steps on the pathway from q-HFeOH + N_2 to q-N_2H_2FeO are 45.3, 6.0, and 50.7 kcal/mol, that is, they are lower than the barriers in the N_2/H_2/BeO system, 62.8, 1.8, and 57.4 kcal/mol, except for the least critical second reaction step. Also, the highest barrier

TABLE 3: ZPE and ZPE-Corrected Relative Energies (kcal/mol) of Various Species in the N_2/H_2/FeO System Calculated at the B3LYP/6-31G and B3LYP/6-311+G(3df,2p) Levels of Theory**

	B3LYP/6-31G**		B3LYP/6-311+G(3df,2p)
species	ZPE	rel energy	rel energy
q-FeO + H_2 + N_2	12.52	0.0	0.0
q-HFeOH + N_2	14.20	−49.54	−46.30
q-TS1	15.07	−13.22	−1.04
q-*cis*-η^2-N_2(H)FeOH	17.45	−13.38	−3.47
q-TS2	16.41	−5.93	2.48
q-*trans*-η^2-N_2(H)FeOH	18.36	−24.45	−13.03
q-TS3	17.50	25.63	37.71
q-N_2H_2FeO	20.71	10.58	25.13
q-FeO + *trans*−HNNH	20.36	45.28	47.08
t-FeO + H_2 + N_2	12.16	22.16	27.91
t-HFeOH + N_2	14.65	−21.60	−15.60
t-N_2Fe(H)OH	17.04	−40.98	−23.57
t-TS1	15.35	−5.79	8.60
t-η^2-N_2(H)FeOH	19.25	−23.11	−9.41
t-TS3	17.74	43.45	54.34
t-N_2H_2FeO	20.39	21.27	34.69
t-FeO + *trans*-HNNH	20.00	67.44	74.99

TABLE 4: Vibrational Frequencies (cm^{-1}) of Various Species in the N_2/H_2/FeO System Calculated at the B3LYP/6-31G Level of Theory**

species	frequencies
q-TS1	783i, 114, 133, 191, 407, 562, 569, 585, 752, 1433, 1897, 3894
q-*cis*-η^2-N_2(H)FeOH	110, 123, 152, 323, 450, 544, 731, 764, 1369, 1612, 2096, 3935
q-TS2	434i, 97, 136, 155, 375, 473, 540, 752, 1249, 1447, 2347, 3906
q-*trans*-η^2-N_2(H)FeOH	87, 120, 166, 344, 459, 496, 520, 753, 1374, 1575, 3035, 3916 q-TS31497, 198, 223, 434, 606, 646, 849, 1326, 1442, 1572, 1755, 3193
q-N_2H_2FeO	107, 109, 287, 470, 517, 977, 1086, 1241, 1359, 1591, 3337, 3404
t-N_2Fe(H)OH	120, 193, 237, 323, 431, 524, 679, 757, 831, 1930, 2013, 3883
t-TS1	1486i, 120, 148, 272, 347, 417, 486, 777, 940, 1523, 1779, 3929
t-η^2-N_2(H)FeOH	107, 155, 337, 413, 535, 553, 572, 775, 1183, 1529, 3375, 3932
t-TS3	1588i, 154, 325, 468, 636, 642, 872, 1340, 1475, 1544, 1785, 3170
t-N_2H_2FeO	52, 158, 285, 408, 617, 906, 975, 1194, 1319, 1543, 3360, 3445

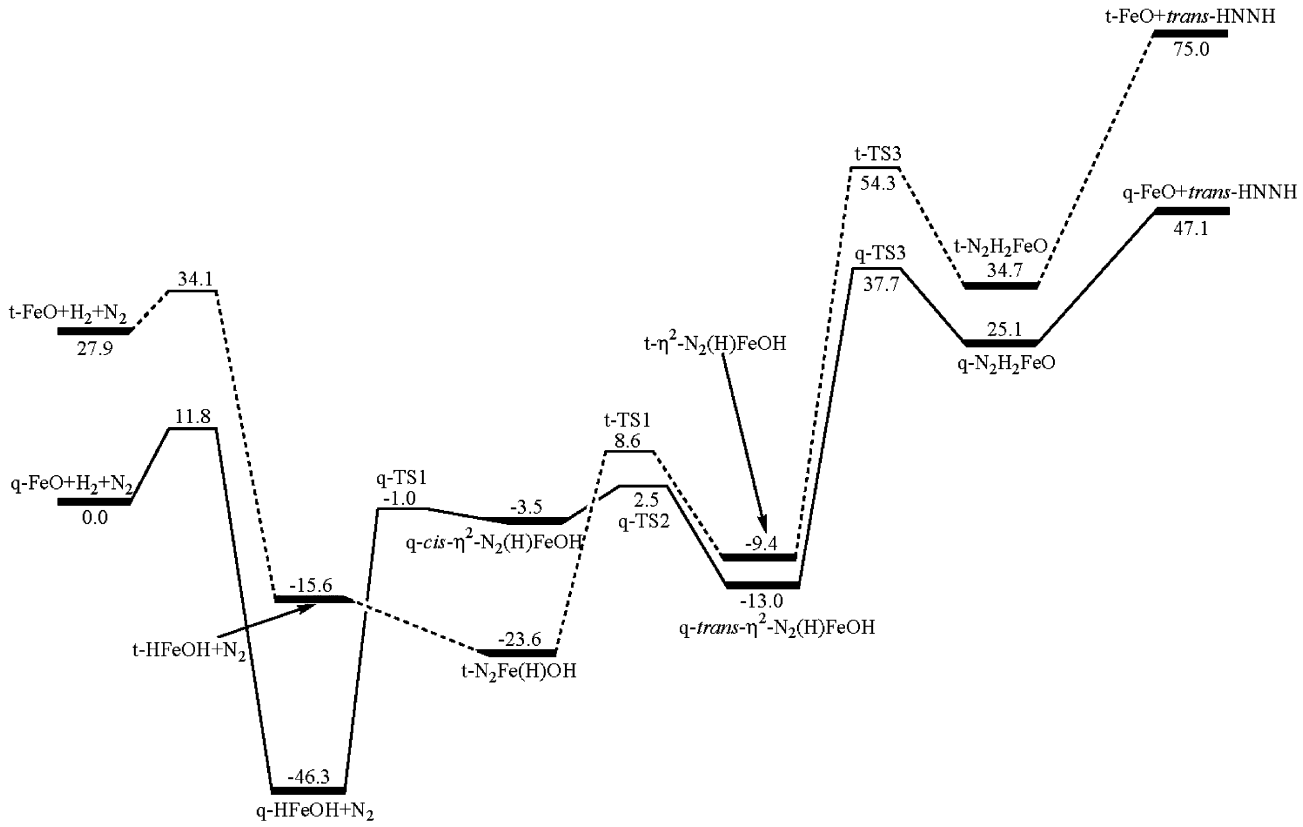

Figure 3. Potential energy diagram of the FeO + H_2 + N_2 → FeO + *trans*-HNNH reaction in quintet and triplet electronic states calculated at the B3LYP/6-311+G(3df,2p)//B3LYP/6-31G** + ZPE(B3LYP/6-31G**) level of theory. All relative energies are given in kcal/mol.

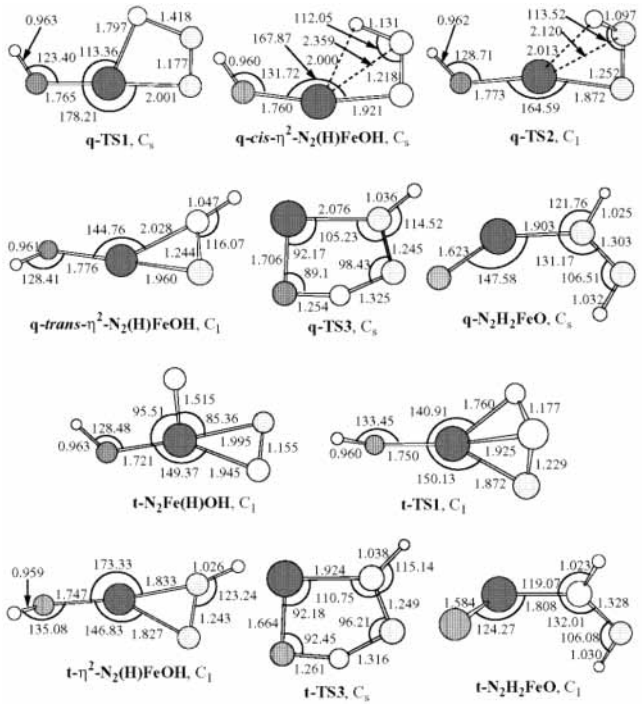

Figure 4. Geometries of intermediates and transition states of the FeO + H_2 + N_2 → FeO + *trans*-HNNH reaction in quintet and triplet electronic states optimized at the B3LYP/6-31G** level of theory. Bond lengths are in Å and bond angles are in deg.

relative to q-HFeOH + N_2 (at q-TS3), 84.0 kcal/mol, is lower than the barrier at TS4 relative to HBeOH + N_2, 90.6 kcal/mol. On the basis of these observations, q-HFeOH should be more efficient in transformation of molecular nitrogen to diazene than HBeOH, although the computed barriers are still rather high. On the other hand, the gas-phase q-FeO + H_2 + N_2 → N_2H_2FeO reaction proceeding through initial formation of q-HFeOH and without collisional deactivation of the latter before it meets N_2 shows the highest barrier of 37.7 kcal/mol relative to the initial reactants (at q-TS3), which is higher than the highest barrier for the BeO + H_2 + N_2 → N_2H_2BeO reaction. This difference owes to the deep potential well at HBeOH, 90.6 kcal/mol relative to BeO + H_2, vs 46.3 kcal/mol for q-HFeOH relative to q-FeO + H_2. The last reaction step, dissociation of the N_2H_2MO complex to *trans*-HNNH and metal oxide, exhibits a lower energy loss for M = Fe than for M = Be. Similarly to the N_2/H_2/BeO system, we can expect that the N_2H_2FeO complex can react with a second H_2 molecule eventually producing N_2H_4FeO and the reaction of the latter with a third H_2 would lead to $2NH_3$ + FeO.

N_2 + H_2 + FeO → trans-N_2H_2 + FeO Reaction in Triplet Electronic State. As can be seen in Figures 3 and 4, the mechanism of the N_2 + H_2 → *trans*-HNNH reaction in the presence of iron oxide in the $^3\Sigma^-$ electronic state has much in common with that for quintet FeO ($^5\Delta$). t-FeO reacts with molecular hydrogen producing t-HFeOH via a barrier of ~6 kcal/mol[27] and with exothermicity of 43.5 kcal/mol. In contrast to the quintet state reaction, t-HFeOH and molecular nitrogen can form a t-N_2Fe(H)OH complex bound by 8.0 kcal/mol. Hydrogen migration from Fe to N in the complex leads to t-η^2-N_2(H)FeOH via a 32.2 kcal/mol barrier, ~13 kcal/mol lower than the corresponding barrier on the quintet state PES. We have found only one nonplanar conformer of t-η^2-N_2(H)FeOH, with the geometry similar to that of q-*trans*-η^2-N_2(H)FeOH, that is, with a three-member FeN_2 ring and without agostic Fe−H bond. In the triplet state, the t-HFeOH + N_2 → t-η^2-N_2(H)-FeOH reaction step is much less endothermic (6.2 kcal/mol) than that in the quintet state (33.3 kcal/mol). The H migration

in t-η^2-N_2(H)FeOH via a five-member ring transition state t-TS3 results in the t-N_2H_2FeO complex. For this step, the barrier in the triplet state, 63.7 kcal/mol, is 13.0 kcal/mol higher than the barrier at q-TS3 on the quintet PES. The complex of diazene with FeO($^3\Sigma^-$), t-N_2H_2FeO, is bound by 40.3 kcal/mol.

The calculations show that although the ground quintet and excited triplet PESs in the N_2/H_2/FeO system may cross each other in the vicinity of q-TS2 and t-TS1, the existence of the excited triplet state is not expected to enhance the HFeOH + N_2 reaction because of the high barrier at t-TS3.

Conclusions

Ab initio and density functional calculations of PESs for the N_2/H_2/BeO and N_2/H_2/FeO systems show that beryllium and iron oxides can enhance the reactions of nitrogen hydrogenation. The mechanism for both reactions involves addition of the hydrogen molecule to metal oxide to form the HMOH species. This process depicts no barrier relative to the reactants for BeO[12] and a relatively low 12−13 kcal/mol barrier for FeO.[27] At the next step, HMOH reacts with molecular nitrogen through N_2 insertion into the M−H bond. Due to the relative weakness of the M−H bonds as compared to H−H, the insertion barrier reduces from 125.2 kcal/mol for the $N_2 + H_2$ reaction[12] to 68.9 and 45.3 kcal/mol for N_2 + HBeOH and N_2 + HFeOH, respectively. After the insertion, cis and trans isomers of the η^2-N_2(H)MOH molecules are formed sequentially. The next reaction step is the H atom migration from O to N in *trans*-η^2-N_2(H)MOH, which takes place via five-member ring transition states and exhibits the barriers of 59.2 and 50.7 kcal/mol for the BeO and FeO systems, respectively. The 1,4-H shift results in the N_2H_2MO complexes of metal oxides with *trans*-diazene bound by 49.8 and 22.0 kcal/mol for M = Be and Fe, respectively. Dissociation of N_2H_2MO to metal oxide and HNNH occurs without exit barriers. Thus, the $N_2 + H_2 \rightarrow$ HNNH reaction can be catalyzed by BeO and FeO because the barriers for individual reaction steps are significantly reduced if the reaction takes place in the presence of the metal oxides. For iron oxide, this barrier reduction is more considerable.

Relative to the HMOH + N_2 species, the highest barriers on the reaction pathways constitute 93.9 and 84.0 kcal/mol for the BeO and FeO reactions, respectively, so the gas-phase HMOH + N_2 reactions are not likely to occur. On the other hand, the MO + H_2 + N_2 reactions in the gas phase are more facile providing that the chemically activated HMOH species formed at the first step do not dissipate their energy through collisions before they meet the N_2 molecule. In this case, BeO is a more efficient catalyst than FeO because the highest barrier on the pathway leading to N_2H_2BeO is only 5.7 kcal/mol relative to BeO + H_2 + N_2 compared to 37.7 kcal/mol for FeO.

In general, the efficiency of nitrogen hydrogenation in the presence of a metal oxide would probably depend on the M−H bond strength, on the ability of the metal to form intramolecular hydrogen (agostic) bond in the NN(H)MOH intermediate, which can reduce the barrier for the N_2 insertion into M−H, and on the deepness of the potential well at HMOH—a lower energy of the latter results in lower barriers with respect to the reactants for the MO + H_2 + $N_2 \rightarrow$ N_2H_2MO reaction but, on the other hand, means higher barriers for individual reaction steps.

The second stage of nitrogen hydrogenation in the presence of BeO is shown to proceed by the H_2 addition to N_2H_2BeO with a barrier of 10.4 kcal/mol to form the HBeOH molecular complex with diazene, HNN(H)Be(H)OH. This is followed by insertion of HNNH into the Be−H bond leading to the H_2NN(H)BeOH intermediate. The H shift transition state lies 19.1 kcal/mol lower in energy than the initial reactants. The second hydrogen in H_2NN(H)BeOH undergoes a 1,3-shift from O to N giving the N_2H_4BeO complex via a transition state, which lies 7.6 kcal/mol below N_2H_2BeO + H_2. Therefore, the highest barrier on the N_2H_2BeO + $H_2 \rightarrow$ N_2H_4BeO reaction pathway is 10.4 kcal/mol for the initial step. The third stage occurs through the N_2H_4BeO + H_2 reaction, which overcomes a 6.8 kcal/mol barrier and leads to the formation of the complex of HBeOH with hydrazine, N_2H_4Be(H)OH. A 1,3-H shift in the latter results in the H_2NBe(NH_3)OH molecule via a barrier of 13.4 kcal/mol relative to N_2H_4BeO + H_2. Next, H_2NBe(NH_3)-OH eliminates ammonia losing 21.6 kcal/mol, and then a 1,3-H shift in H_2NBeOH leads to the formation of the H_3NBeO complex via transition state located 23.1 kcal/mol lower in energy than N_2H_4BeO + H_2. Finally, H_3NBeO can dissociate to NH_3 and beryllium oxide without an exit barrier, and the total endothermicity of the N_2H_4BeO + $H_2 \rightarrow$ $2NH_3$ +BeO reaction is 13.3 kcal/mol. Thus, the highest barrier for the third stage of BeO-catalyzed nitrogen hydrogenation is 13.4 kcal/mol. These results indicate that the N_2H_2MO and N_2H_4MO complexes can react with H_2 molecules eventually leading to the $2NH_3$ + MO products.

Acknowledgment. Funding from Tamkang University was used to buy the computer equipment used in part of this investigation. A partial support from Academia Sinica and from the National Science Council of Taiwan, R.O.C., is also appreciated.

References and Notes

(1) Büchel, H.; Moretto, H.-H.; Woditsch, P. *Industrielle Anorganische Chemie*; Wiley/VCH: Weinheim, Germany, 1999; Vol. 3.
(2) McBryde, A. E. In *Nobel Laureates in Chemistry*; James, L. K., Ed.; American Chemical Society and Chemical Heritage Foundation: Washington, DC, 1993.
(3) Logadottir, A.; Rod, T. H.; Nørskov, J. K.; Hammer, B.; Dahl, S.; Jacobsen, C. J. H. *J. Catal.* **2001**, *197*, 227.
(4) Aika, K.; Ozaki, A. *Catal. Sci. Technol.* **1981**, *1*, 87.
(5) Emmett, P. H.; Brunauer, S. *J. Am. Chem. Soc.* **1933**, *55*, 1738.
(6) Ertl, G.; Huber, M.; Lee, S. B.; Paal, Z.; Weiss, M. *Appl. Surf. Sci.* **1981**, *8*, 373.
(7) Jacobsen, C. J. H.; Dahl, S.; Clausen, B. S.; Bahn, S.; Logadottir, A.; Nørskov, J. K. *J. Am. Chem. Soc.* **2001**, *123*, 8404.
(8) Hammer, B. *Phys. Rev. B* **2001**, *63*, 205423.
(9) Hwang, D.-Y.; Mebel, A. M. *J. Phys. Chem. A* **2003**, *107*, 2865.
(10) Nicolaides, C. A.; Valtazanos, P. *Chem. Phys. Lett.* **1991**, *176*, 239.
(11) Valtazanos, P.; Nicolaides, C. A. *J. Chem. Phys.* **1993**, *98*, 549.
(12) Hwang, D.-Y.; Mebel, A. M. *Chem. Phys. Lett.* **2000**, *321*, 95.
(13) Hwang, D.-Y.; Mebel, A. M. *J. Phys. Chem. A* **2001**, *105*, 10433.
(14) Hehre, W. J.; Radom, L.; Schleyer, P. v. R.; Pople, J. A. *Ab Initio Molecular Orbital Theory*; Wiley: New York, 1986.
(15) Gonzales, C.; Schlegel, H. B. *J. Chem. Phys.* **1989**, *90*, 2154.
(16) Scott, A. P.; Radom, L. *J. Phys. Chem.* **1996**, *100*, 16502.
(17) Mebel, A. M.; Morokuma, K.; Lin, M. C. *J. Chem. Phys.* **1995**, *103*, 7414.
(18) Curtiss, L. A.; Raghavachari, K.; Trucks, G. W.; Pople, J. A. *J. Chem. Phys.* **1991**, *94*, 7221.
(19) Pople, J. A.; Head-Gordon, M.; Fox, D. J.; Raghavachari, K.; Curtiss, L. A. *J. Chem. Phys.* **1989**, *90*, 5622.
(20) Curtiss, L. A.; Jones, C.; Trucks, G. W.; Raghavachari, K.; Pople, J. A. *J. Chem. Phys.* **1990**, *93*, 2537.
(21) Curtiss, L. A.; Raghavachari, K.; Pople, J. A. *J. Chem. Phys.* **1993**, *98*, 5523.
(22) Purvis, G. D.; Bartlett, R. J. *J. Chem. Phys.* **1982**, *76*, 1910.
(23) Becke, A. D. *J. Chem. Phys.* **1993**, *98*, 5648.
(24) Lee, C.; Yang, W.; Parr, R. G. *Phys. Rev. B* **1988**, *37*, 785.
(25) Torrent, M.; Solà, M.; Frenking, G. *Chem. Rev.* **2000**, *100*, 439.
(26) Glukhovtsev, M. N.; Bach, R. D.; Nagel, C. J. *J. Phys. Chem. A* **1997**, *101*, 316.
(27) Hwang, D.-Y.; Mebel, A. M. *J. Phys. Chem. A* **2001**, *105*, 7460.
(28) Werner, H.-J.; Knowles, P. J. *J. Chem. Phys.* **1988**, *89*, 5803.
(29) Knowles, P. J.; Werner, H.-J. *Chem. Phys. Lett.* **1988**, *145*, 514.
(30) Moore, S. E. *Atomic Energy Levels*; NSRDS: Washington, DC, 1971.

(31) Frisch, M. J.; Trucks, G. W.; Schlegel, H. B.; Scuseria, G. E.; Robb, M. A.; Cheeseman, J. R.; Zakrzewski, V. G.; Montgomery, J. A., Jr.; Stratmann, R. E.; Burant, J. C.; Dapprich, S.; Millam, J. M.; Daniels, A. D.; Kudin, K. N.; Strain, M. C.; Farkas, O.; Tomasi, J.; Barone, V.; Cossi, M.; Cammi, R.; Mennucci, B.; Pomelli, C.; Adamo, C.; Clifford, S.; Ochterski, J.; Petersson, G. A.; Ayala, P. Y.; Cui, Q.; Morokuma, K.; Malick, D. K.; Rabuck, A. D.; Raghavachari, K.; Foresman, J. B.; Cioslowski, J.; Ortiz, J. V.; Stefanov, B. B.; Liu, G.; Liashenko, A.; Piskorz, P.; Komaromi, I.; Gomperts, R.; Martin, R. L.; Fox, D. J.; Keith, T.; Al-Laham, M. A.; Peng, C. Y.; Nanayakkara, A.; Gonzalez, C.; Challacombe, M.; Gill, P. M. W.; Johnson, B. G.; Chen, W.; Wong, M. W.; Andres, J. L.; Head-Gordon, M.; Replogle, E. S.; Pople, J. A. *Gaussian 98*, revision A.7; Gaussian, Inc.: Pittsburgh, PA, 1998.

(32) MOLPRO is a package of ab initio programs written by Werner, H.-J.; Knowles, P. J. with contributions from Almlöf, J.; Amos, R. D.; Deegan, M. J. O.; Elbert, S. T.; Hampel, C.; Meyer, W.; Peterson, K.; Pitzer, R.; Stone, A. J.; Taylor, P. R.; Lindh, R.

(33) Frenking, G.; Koch, W.; Collins, J. R. *J. Chem. Soc., Chem. Commun.* **1988**, 1147.

(34) *CRC Handbook of Chemistry and Physics*, 75th ed.; Lide, D. R., Ed.; CRC Press: Boca Raton, FL, 1995.

(35) *NIST Chemistry Webbook*, February 2000 release; NIST Standard Reference Data Base Number 69; National Institute of Standards and Technology: Washington, DC, 2000 (http://webbook.nist.gov/chemistry/).